รายงานวิจัยฉบับสมบูรณ์

โครงการการส่งผ่านการสั่นสะเทือนจากวงแหวนขดลวดเหนี่ยวนำสู่ฐานของสปินเดิลมอเตอร์สำหรับฮาร์ดดิสก์ไดร์ฟ

โดย ผศ.ดร. นภดนัย อาชวาคม

เมษายน 2558

สัญญาเลขที่ MRG5380169

รายงานวิจัยฉบับสมบูรณ์

โครงการการส่งผ่านการสั่นสะเทือนจากวงแหวนขดลวดเหนี่ยวนำสู่ฐาน ของสปินเดิลมอเตอร์สำหรับฮาร์ดดิสก์ไดร์ฟ

ผู้วิจัย สังกัด

ผศ.ดร. นภดนัย อาชวาคม คณะวิศวกรรมศาสตร์ จุฬาลงกรณ์มหาวิทยาลัย

สนับสนุนโดยสำนักงานคณะกรรมการการอุดมศึกษา สำนักงานกองทุนสนับสนุนการวิจัย และ จุฬาลงกรณ์มหาวิทยาลัย

1. บทคัดย่อภาษาไทย และภาษาอังกฤษ

บทคัดย่อ

รหัสโครงการ: MRG5380169

ชื่อโครงการ: การส่งผ่านการสั่นสะเทือนจากวงแหวนขดลวดเหนี่ยวนำสู่ฐานของสปินเดิลมอเตอร์สำหรับฮาร์ดดิสก์ไดร์ฟ

ชื่อนักวิจัย และสถาบัน ผศ.ดร. นภดนัย อาชวาคม คณะวิศวกรรมศาสตร์ จุฬาลงกรณ์มหาวิทยาลัย

อีเมล์: nopdanai@chula.ac.th

ระยะเวลาโครงการ: 2 ปี (มิถุนายน 2553 ถึง มิถุนายน 2555)

บทคัดย่อ:

โครงการวิจัยนี้ได้ศึกษากลไกและผลของค่าการสวมอัดแบบแน่น (Interference fit) ระหว่างแบบจำลองของวงแหวนขดลวดเหนี่ยวนำและฐานของสปินเดิลมอเตอร์ต่อการส่งผ่านการสั่นสะเทือนระหว่างส่วนประกอบทั้งสองในช่วงความถี่ที่หูของมุนษย์สามารถได้ยิน คือ 0 – 20 kHz โดยนำหลักการ Statistical energy analysis มาช่วยวิเคราะห์ผลในการทดสอบ ผลที่ได้จะช่วยทำให้เข้าใจผลของค่า Interference fit ต่าง ๆ กันต่อการส่งผ่านการสั่นสะเทือนระหว่างส่วนประกอบทั้งสองและสามารถนำเสนอแนวทางในการวิเคราะห์เพื่อให้ได้ผลที่ถูกต้องแม่นยำต่อไป โดยงานวิจัยนี้จะเริ่มจากการนำแบบจำลองของวงแหวนขดลวดเหนี่ยวนำและฐานของสปินเดิลมอเตอร์จำนวนหลายชุดซึ่งมีค่า Interference fit ต่าง ๆ กันมากระตุ้นด้วยค้อนเคาะและเครื่องกำเนิดแรงสั่นสะเทือน ค่าการสั่นสะเทือนที่วัดได้จาก Accelerometer และเครื่อง Laser Doppler Vibrometer ที่ตำแหน่งต่าง ๆ จะนำมาใช้ในการคำนวณหาค่า Intrinsic loss factor และ Coupling loss factor ตามหลักการของ Statistical energy analysis และนำไปใช้ในการหาค่ากำลังการสั่นสะเทือนรวมที่ถูกส่งผ่านจากแบบจำลองของวงแหวนขดลวดเหนี่ยวนำสู่ฐานของสปินเดิลมอเตอร์ของแบบจำลองแต่ละชุด และนำมาเปรียบเทียบระหว่างกันเพื่อหาความสัมพันธ์ของค่า Interference fit ต่อการส่งผ่านการสั่นสะเทือนระหว่างส่วนประกอบทั้งสองต่อไป จากผลการทดสอบ พบว่าในช่วงความถี่ต่ำและความถี่กลาง เมื่อค่า Interference fit ระหว่างแบบจำลองของวงแหวนขดลวดเหนี่ยวนำและฐานของสปินเดิลมอเตอร์มีค่าลดลง จะส่งผลทำให้ค่ากำลังการส่งผ่านการสั่นสะเทือนรวมระหว่างส่วนประกอบทั้งสองมีค่าลดต่ำลงและเพิ่มสูงขึ้น ตามลำดับ โดยเมื่อค่า Interference fit ลดลงต่ำกว่าค่าหนึ่ง จะส่งผลทำให้ค่ากำลังการส่งผ่านการสั่นสะเทือนรวมในช่วงความถี่ต่ำและช่วงความถี่กลาง จะมีค่าเพิ่มสูงขึ้น

และลดต่ำลง ตามลำดับ โดยผลที่ได้นี้สามารถนำไปประยุกต์ใช้ในการลดการสั่นสะเทือนที่ส่งผ่านสู่ภายนอกฮาร์ดดิสก์ไดร์ฟได้ต่อไป

คำหลัก : การวิเคราะห์สถิติพลังงาน การสวมอัด สปินเดิลมอเตอร์

Abstract

Project Code: MRG5380169

Project Title: Vibrational Energy Transmission from Stator Coil to Base of Spindle Motor in Hard Disk Drive

Investigator: Assistant Professor Nopdanai Ajavakom

E-mail Address: nopdanai@chula.ac.th

Project Period: 2 years (June 2010 to June 2012)

Abstract:

This research projects aims to study the mechanism and effect of interference fit on vibration transmission between the model of stator and base in human audible frequency range (0 – 20 kHz) by using statistical energy analysis approach to analyze the experimental results. The results will explain the effect of interference fit on vibration transmission between two components and present the analytical approach that will lead to the accurate results. The experiment started with the excitation of various interference fit models of spindle motor, the combination of stator and base, by impact hammer and vibration exciter. After the excitation, the vibrational values measured from accelerometer and Laser Doppler Vibrometer were used in calculations of intrinsic loss factor, coupling loss factor and total vibration transmission power from stator to base using the statistical energy analysis approach. Finally, the results from the calculations of each model would be compared in order to study the effect of interference fit on vibration transmission between the model of stator and base. The experimental results show that the less interference fit leads to the less vibrational power transmitted from the model of stator to base for low frequency range but more vibration power medium frequency range. After the interference fit is below one point, the effect will be reversed, more and less power transmission for low and medium frequency range respectively. All results can be applied to be an approach in reduction of the transmitted vibration from inner to outer of hard disk drive in further study.

Keywords: Statistical Energy Analysis, Interference fit, Spindle Motor, Coupling Loss Factor

2. Executive summary

This research aims to present the application of an energy-based method, Statistical Energy Analysis, in the study of an effect of the interference fit on vibrational transmission between the stator and the base in spindle motor which is the origin of the vibration in hard disk drive. In this application, the model of stator-base was separated into two subsystems which exchanged energy with each other. The measured vibrational variables, which were measured from excitation of the stator-base models by the vibration exciter, were used in calculations of coupling loss factor and transmitted vibrational power from the stator to the base of each model. The experimental results show that the less interference fit means the less transmitted vibrational power from the stator to the base.

3. Objectives

1. Identify the mechanism of vibration generation inside the spindle motor and the path of vibration transmission from the inside to the outside of the motor.
2. Analyze the relation between the transmitted vibrational energy and the interference fit of the stator and the base of the spindle motor.
3. Propose an approach of modification of interference fit between the stator and the base to reduce vibration transmitted to the base plate.

4. Introduction

A hard disk drive (HDD) is an important component in a personal computer to store the data. In need of higher performance HDDs including higher capacity, faster data read/write time, quieter operation while maintaining or even reducing the HDD physical size, the spindle motors are required to spin faster and smoother. Thus, the vibration transmitting from the interior to the exterior of the spindle motor, which may finally cause the data read/write errors and the emission the acoustic noise, has to be looked into. The primary source of vibration inside the motor is the electromagnetic (EM) sources, not the mechanical unbalance of the moving parts [1,2]. The EM sources are originated from the physical and the electromagnetic designs of the permanent magnet ring and the stator teeth of the motor as well as the characteristics of the input power from the motor inverter. The designs contribute the unbalance radial, tangential, and axial forces on the permanent magnet ring and the stator teeth deforming the interior

structure of the motor. The deformations of the stator teeth, especially from varying tangential forces (torque ripple), are transmitted to the base bracket via the cylindrical-shell sleeve causing transverse vibration of the base plate [3]. Moreover, the deformations of the ring propagate into rotor hub as transverse and radial vibrations [3]. The vibrations of the motor exterior are responsible for the acoustic noise emitted from the motor. The approaches to decrease the vibrations and the acoustic noise from the motor include the elimination of EM sources, modification of the motor physical design to minimize the sound radiation, and reduction of the vibration transmission from the motor interior to the exterior, such as by optimizing the interference fit between the stator coil and the base bracket, see Fig.1.

This project focuses on the effect of interference fit between the stator coil and the base of the spindle motor on the torsional vibrational energy transmission from the stator coil to the base plate aiming to reduce the transmitted energy capable of the motor's exterior vibrations and the emitted acoustic noise. The article contains both vibration energy transmission analysis and two experimental investigations.

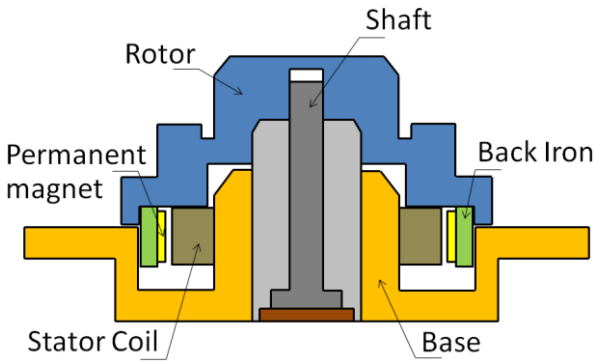

Fig. 1 Cross-section view of a spindle motor showing the fit between the stator coil and the base bracket

5. Vibrational Energy Transmission Analysis

The analysis of vibrational energy transmission between the stator coil and the base of the motor involves a friction model and vibration transmission mechanism of the two surfaces in contact with the clamping pressure. Jintanawan et al. [4] study a simple dynamic model of the stator coil and the base of a spindle motor featuring the two-degree of freedom lumped mass model with attached to a fixed foundation via a torsional spring. The Dahl's model is used to analyze the relative angular displacement

between the two components due to the applied impulsive torque at the stator coil. The study shows that the more interference fit the more vibrational energy transmitted to the base and vice versa.

Nevertheless, for the continuous and more complex system, such as the spindle motor, the analysis that considers the internal forces on the surfaces, the micro-slip, the pre-sliding behavior, and the force's loading-unloading-reloading stages is more suitable. Such analysis as that by Metherell and Diller [5] is modified to work on a stator-base model of a spindle motor. It will be shown from the hysteresis diagram of the torque versus the relative angular displacement that the vibrational energy loss is lower (the energy transmission is higher) as the interference fit is more.

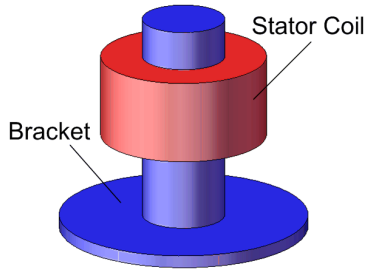

Fig. 2 Simple model of stator and base bracket

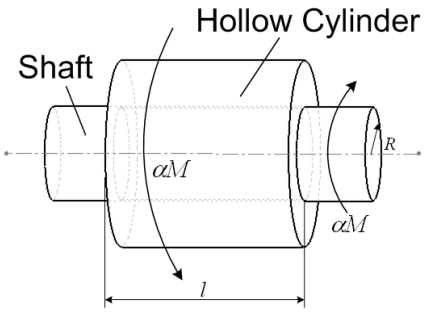

Fig. 3 Dynamic model of stator and base

Consider the simplified stator-base model shown in Fig. 2 where the stator is a ring press-fit into the base bracket via a sleeve. To simplify the analysis, the sleeve is assumed to be a solid shaft of radius R and the ring is assumed to be a hollow cylinder of length l shown in the dynamic model in Fig. 3. Torques are applied to the left side of the cylinder and the right side of the shaft. They are opposite with the equal magnitude of αM, where $0 \le \alpha \le 1$, preventing any angular displacement of the whole assembly. The micro-slip is taken into account and the concept of Coulomb friction is

used, the torsional friction per unit length of the cylinder on the contact surfaces is then

$$m = 2\pi\mu PR^2, \tag{1}$$

where m is the torsional friction per unit length (N-m/m), μ is coefficient of friction, P is the pressure between the cylinder and the shaft due to the fit (Pa), and R is the radius of the shaft (m). In our case, according to Eq. (1), the torsional friction per unit length is, in general, constant over the length of the cylinder due to the constant interference fit pressure, coefficient of friction and radius of the shaft. In one cycle of the varying applied torque, the torque is exerted to the model in three non-stop consecutive stages: loading, unloading, and reloading.

In the loading stage, the applied torque on the cylinder increases from 0 to M, that is αM, where α increases from 0 to 1. At the same time, the resisting torque at the shaft increases to balance out the applied torque creating friction on the contact surfaces. The diagrams of the torsional friction per unit length, internal torsion on the cylinder surface, and the internal torsion on the shaft surface are shown in Fig. 4. The torsional friction per unit length is m with the exception of being zero in the middle region of the length of the cylinder where there is no slipping. The slipping and the torsional friction occur at the left and right edge of the contact surfaces with length on each side equals a_1 $(0 < a_1 < l/2)$, where a_1 depends on the magnitude of the applied torque. The internal torsion on the cylinder surface is αM at the left edge and it decreases with the slope $-m$ as it goes to the right. Likewise, the internal torsion at the shaft surface is αM at the right edge and decrease with the slope $-m$ as it goes to the left. In addition, the summation of internal torsions at the cylinder and the shaft surfaces must be equal to αM along the length of the cylinder.

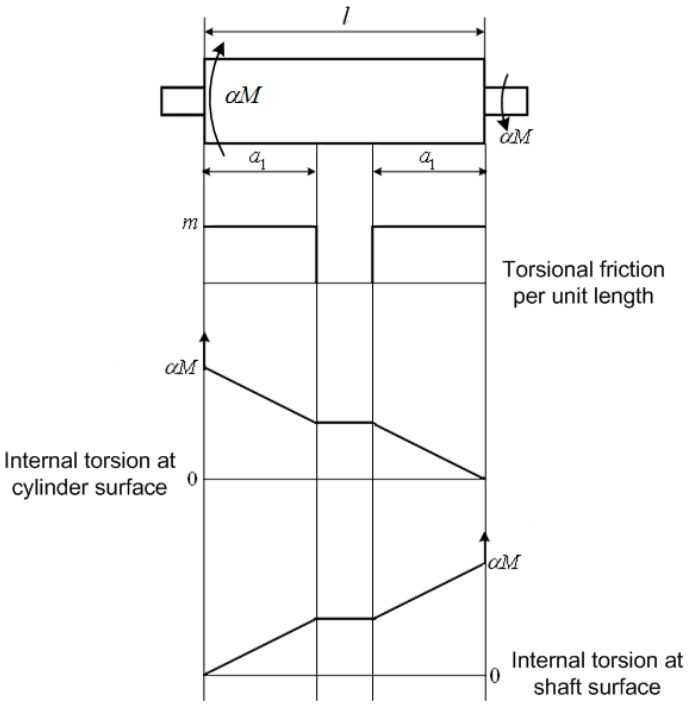

Fig. 4 Loading stage diagram

In the unloading stage, being reverse to the loading stage, the applied torque αM on the cylinder now decreases from M to rM as α decreases from 1 to r, where r is constant and $0 \le r < 1$. Since the applied torque decreases, the torsional friction per unit length is now $-m$ making the internal torsion on the cylinder surface increases with the slope m as it goes to the left. The phenomenon is called "counter slip." The counter slip occurs for the length of a_2. The further inside region of the cylinder and the shaft still experiences the torsional friction m remaining from the loading stage. The diagrams of the torsional friction per unit length, internal torsion on the cylinder surface, and the internal torsion on the shaft surface for the unloading stage are shown in Fig. 5.

In the reloading stage, being quite similar to the loading stage and reverse to the unloading stage, the applied torque αM on the cylinder increases back from rM to M as α increases from r to 1, where $0 \le r < 1$. The torsional friction per unit length currently returns to m at the left and right sides of the cylinder. The diagrams of the torsional friction per unit length, internal torsion on the cylinder surface, and the internal torsion on the shaft surface of the reloading stage are shown in Fig. 6.

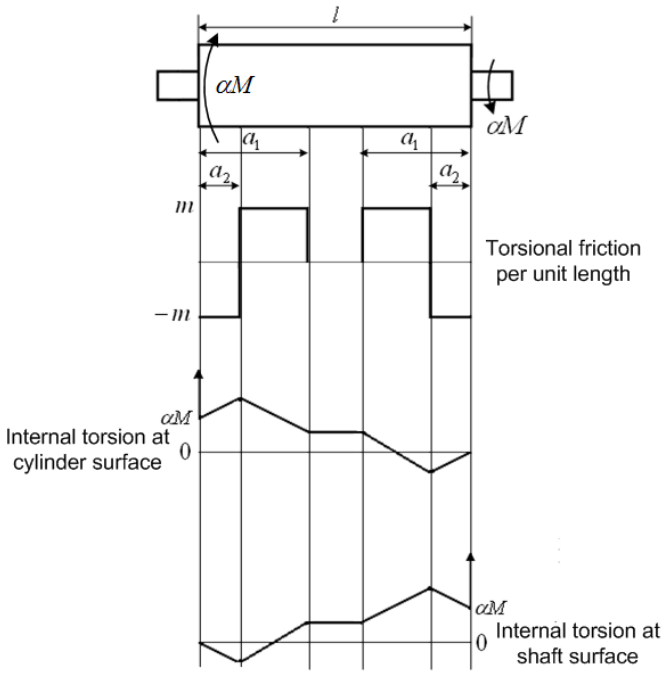

Fig. 5 Unloading stage diagram

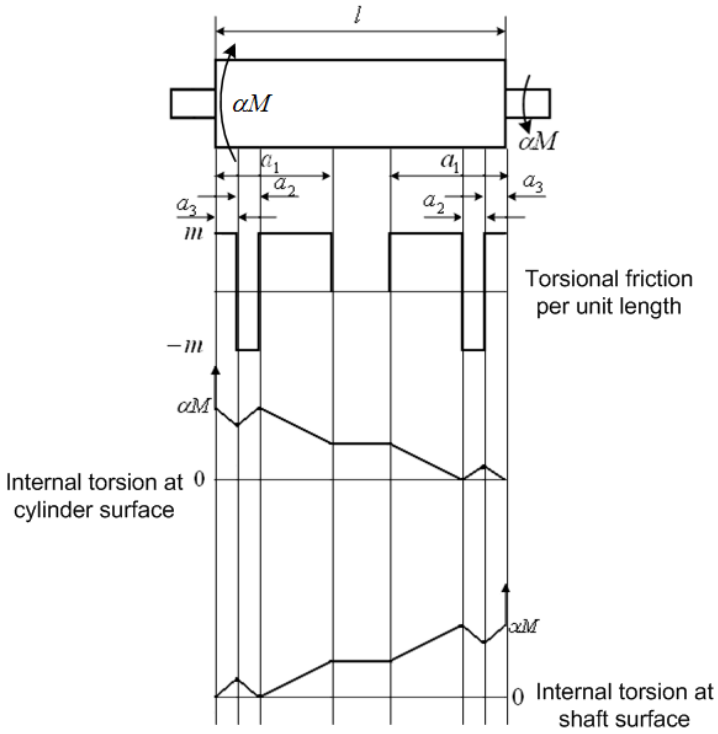

Fig. 6 Reloading stage diagram

The relative angular displacement of each stage can be determined from the torsional friction per unit length, the internal torsions on the surfaces, the shaft's and the cylinder's material properties, and other previously introduced constants:

$$\phi_1 = \frac{k\alpha Ml}{G_s I_s} + \frac{\left(1-3k+3k^2\right)\alpha^2 M^2}{2mG_s I_s\left(1-k\right)}, \qquad 0 < \alpha < 1 \qquad (2)$$

$$\phi_2 = \frac{k\alpha Ml}{G_s I_s} + \frac{M^2\left(1+2\alpha-\alpha^2\right)\left(1-3k+3k^2\right)}{4mG_s I_s\left(1-k\right)}, \qquad 0 \le r < \alpha < 1 \qquad (3)$$

$$\phi_3 = \frac{k\alpha Ml}{G_s I_s} + \frac{M^2\left(1+2r-\alpha^2-2\alpha r\right)\left(1-3k+3k^2\right)}{4mG_s I_s\left(1-k\right)}, \qquad 0 \le r < \alpha < 1 \qquad (4)$$

$$k = \frac{G_s I_s}{G_s I_s + G_c I_c} \qquad (5)$$

where ϕ_1, ϕ_2, ϕ_3 are the relative angular displacements for the loading, unloading, and reloading stages, respectively, $G_c I_c$ and $G_s I_s$ are the torsional stiffness of the cylinder and the shaft, respectively, and k is the combined torsional stiffness of the cylinder and the shaft. The angular displacements can be plotted against α to form a hysteresis loop depicted in Fig. 7.

The transmission energy loss due to the friction of the fit can be obtained from the area enclosed by the relative angular displacements under the three stages over one cycle,

$$\psi = \frac{2M_a^3\left(1-3k+3k^2\right)}{3mG_s I_s\left(1-k\right)} \qquad (6)$$

where ψ is the energy loss due to friction (J) and

$$M_a = \frac{1}{2}M\left(1-r\right), \qquad 0 < r < 1 \qquad (7)$$

According to Eqs. (6) and (7), the transmission energy loss depends on the cube of the applied torque and inversely depends on the torsional friction per unit length given that the other parameters are constant. Focusing on the effect of the interference fit, the equations indicate that the energy loss is less when the torsional friction is larger because of the more pressure from the tighter interference fit, Eq. (1). That is the transmitted vibrational energy from the stator to the base would be more if the interference fit increases. This statement can also be testified by experimental investigations in the next section.

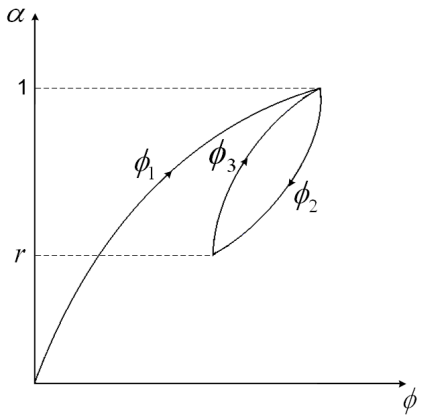

Fig. 7 Hysteresis loop of the dynamic model

6. Experimental Investigations

The experimental investigations are performed to testify the analytical results in the previous section. Sets of simple models of stator coil and base and 3.5-inch HDD spindle motor samples with various fits are made and tested in Sections 6.1 and 6.2, respectively. The tests were done on the simple models first and on motor samples later.

6.1 On simple models of stator coil and base

Three sets of 1.5x-size model of stator coil and base (see Fig. 8) with three interference fits, 0.0083 mm (minimum fit), 0.0169 mm (medium fit) and 0.0304 mm (maximum fit), are tested for the energy transmitted from the stator to the base. The transmission of energy between two systems, stator (system 1) and base (system 2), is analyzed by using Statistical Energy Analysis (SEA) [6, 7]. The power flow diagram is shown in Fig. 9. The input power P_1 from the impact force exerted by the impact hammer at the stator model will go to raise the stator model internal energy W_1, which is related to the power loss to the environment P_{11} and the power transmitted to the base model P_{12}. The power loss P_{11} is

$$P_{11} = \omega \eta_1 W_1, \tag{8}$$

where ω is the frequency and η_1 is the intrinsic loss factor. The transmitted power P_{12} is

$$P_{12} = \omega \eta_{12} W_1, \tag{9}$$

where η_{12} is the coupling loss factor from stator to base. The power equation of the stator model is then

$$P_1 = P_{11} + P_{12} - P_{21}, \tag{10}$$

where P_{21} is the power received from the base. This power also depends on the base model internal energy W_2 and

$$P_{21} = \omega\eta_{21} W_2, \tag{11}$$

where η_{21} is the coupling loss factor from base to stator. Applying the same concept to base model where there is no direct input power from the impact hammer, the power equation of the base model is thus

$$0 = P_{22} + P_{21} - P_{12}, \tag{12}$$

where P_{22} is the power loss to the environment and

$$P_{22} = \omega\eta_{2} W_2, \tag{13}$$

where η_2 is the intrinsic loss factor of system 2.

The approach to determine the transmitted power P_{12} starts with tests to find the intrinsic loss factor of each of the two systems. The test is performed on each system separately, i.e. the stator model has not yet fit into the base model, where P_{12} and P_{21} are non-existent and

$$P_1 = P_{11} = \omega\eta_1 W_1. \tag{14}$$

The stator is then press-fit into the base. In order to simplify the testing for the power transmission, the base is damped out by attaching it to the large mass for minimizing W_2 and thus P_{21} is near zero according to Eq. (11). With the known input power P_1, the intrinsic loss factors η_1, η_2, the coupling loss factor η_{12} as well as the transmitted power P_{12} can be calculated. With the roughly equal input power P_1 of approximately 1.11×10^{-4} W, the transmitted power P_{12} over the 20-kHz span for all three sets with three different interference fits is shown in Fig. 10 and summarized in Table 1 with three equal ranges of frequencies. It can be observed that by roughly looking at the graph in Fig. 10 the system with the maximum interference fit has the largest transmitted power among three systems at the frequency above 12 kHz. At the frequency below 12 kHz, the lines, however, are not smooth, which is suspected to be from some human uncertainties in the experiment, e.g. from the uneven impact force from the hammer. The numerical results for each set in the frequency ranges listed in Table 1 also indicate the similar trend. For the medium and high frequency ranges, the maximum fit set has more transmitted power than the other two sets. The medium fit set has more transmitted power than the minimum fit set. In short, generally speaking,

the system with less fit possesses less transmitted power. This agrees with the analytical results proved in Section 5.

Fig. 8 Assembled simple stator-base model

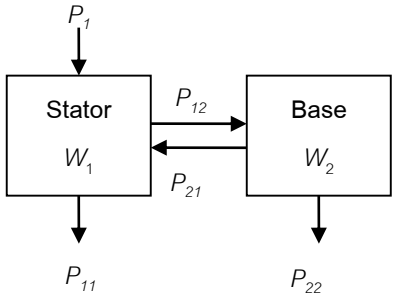

Fig. 9 Power transmission diagram of two systems

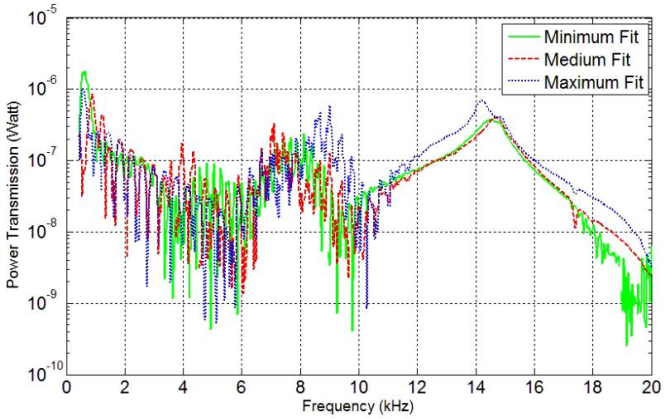

Fig. 10 Transmitted power from stator to base for three interference fits

Table 1 Power transmitted to the base with different interference fits (simple models)

Frequency range/Model fit	Transmitted power (W)		
	Minimum (8.3 μm)	Medium (16.9 μm)	Maximum (30.4 μm)
Low (0-6.6 kHz)	1.45	1.69	1.12
Medium (6.7-13.3 kHz)	1.40	1.34	2.44
High (13.4-20 kHz)	2.05	2.09	3.26
Overall (0-20 kHz)	4.90	5.12	6.82

6.2 On 3.5-inch hard disk drive spindle motors

Two groups of 3.5-inch HDD spindle motors, 3-phase permanent magnet synchronous motors (PMSMs), with different interference fits; Group A with 0.016-and 0.018-mm fits (low fit) and Group B with 0.034-mm fit (high fit), are tested to investigate the effects of stator-base interference fit on the transmitted energy. The varying frequency sinusoidal current is fed into only one phase winding of the spindle motor to excite the stator coil and the rotor structures without spinning the rotor. Particularly, the induced vibration of the stator coil is transmitted to the base plate where the transverse vibrations of 10 various points are measured for calculating the vibrational energy of the base. The transmitted vibrational energy is determined from the spatial average square velocity from the measure points and shown in joules per kg of mass per ampere of the current input in Fig. 11 over a 20-kHz span.

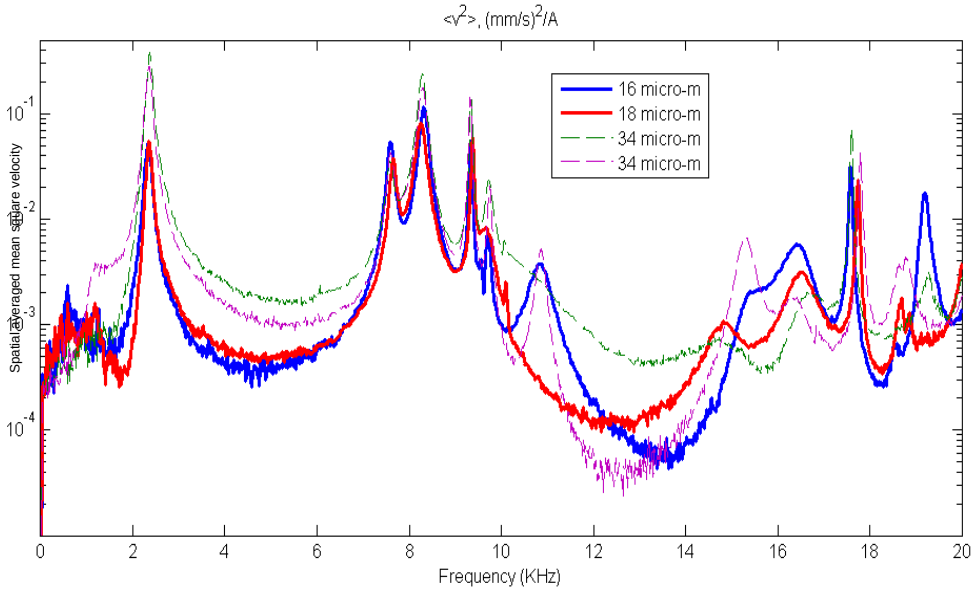

Fig. 11 Vibrational energy of spindle motors with different interference fits

The transmitted vibrational energies are also listed in Table 2 for three equal ranges of frequencies. The results indicate that the vibrational energy over the low, the medium, the high, and the overall frequency ranges of the motors with less fit (Group A) is much lower than that of the motors with more fit (Group B) especially at the low frequency range. The motors with less interference fit between the stator and the base has less transmitted vibrational energy from the stator to the base than those with more interference fit. These experimental results agree quite well with those from Section 3.1 and the analytical ones in Section 5.

7. Conclusion

The effect of interference fit on vibration transmission from stator coil to base of a spindle motor in a hard disk drive has been studied both analytically and experimentally. The analysis of transmission energy loss reveals that the energy loss inversely depends on the pressure from the interference fit. Less energy loss and thus more transmitted energy from the stator to the base are the results of the more interference fit. The experimental investigations on both assembled models of the stator and the base and the spindle motor samples with various fits are carried out and their results agree well with the analysis. Hence, reducing the interference fit at the stator-base assembly in the spindle motor is a promising approach to reduce the

transmitted vibrational energy to the base bracket, and the acoustic noises emitting from the motor should be lower.

Table 2 Vibrational energy transmitted to the base with different interference fits (HDD spindle motors)

Frequency range/Motor group	Vibrational energy (μJ/kg/A)	
	A (16-18 μm)	*B* (34 μm)
Low (0-6.6 kHz)	1.164	6.067
Medium (6.7-13.3 kHz)	4.063	7.263
High (13.4-20 kHz)	0.938	1.004
Overall (0-20 kHz)	6.164	14.33

References

[1] Ajavakom, A., Jintanawan, T., Singhatanagid, P. and Sripakagorn, P. (2007). On investigation of vibro-acoustics of FDB spindle motors for hard disk drives, *Microsystem Technologies,* vol. 13(8-10), May 2007, pp. 1281-1287.

[2] Lin, S., Jiang, Q., Mamun, A.A. and Bi, C. (2003). Effects of drive modes on the acoustic noise of fluid dynamic bearing spindle motors, *IEEE Transactions on Magnetics,* vol. 39, September 2003, pp. 3277-3279.

[3] Jintanawan, T., Sillapapinij, A. and Ajavakom, N. (2009). Effects of tolerance design on suppression of electromagnetic-induced acoustic noises and vibration transmission in hard disk drive spindle motors, *IEEE Transactions on Magnetics,* vol. 45(11), November 2009, pp. 5129-5134.

[4] Jintanawan, T., Chungphaisan, K., Liwcharoenchai, K., Junkaew, P. and Singhatanagid, P. (2007). Role of stator-base interference fit on vibration transmission and acoustic noise in FDB spindle motors for HDD, paper presented in *Proceedings of Information Storage Processing System Conference,* June 2007.

[5] Metherell, A.F. and Diller, S.V. (1968). Instantaneous energy dissipation rate in a lap joint, *Journal of Applied Mechanics,* vol. 35, March 1968, pp. 123-128.
[6] Lyon, R.H. (1975). *Statistical Energy Analysis of Dynamical Systems: Theory and Applications,* The MIT Press Cambridge, Massachusetts, and London, England.
[7] Sarradj, E. (2004). *Energy – based Vibroacoustics: SEA and Beyond*, Gesellschaft für Akustikforschung Dresden mbH, D-01099 Dresden, Germany.

Output จากโครงการวิจัยที่ได้รับทุนจาก สกว.

1. ผลงานตีพิมพ์ในวารสารวิชาการนานาชาติ ที่มี Impact factor
   - Statistical Energy Analysis on Vibrational Energy Transmission in Hard Disk Drive Components ในวารสาร Microsystem Technologies เล่มที่ 20 ฉบับที่ 8-9 เดือน สิงหาคม ปี 2014 เลขหน้า 1753-1760 มี Impact factor 0.952.
2. การนำผลงานวิจัยไปใช้ประโยชน์
   - เชิงวิชาการ (มีการพัฒนาการเรียนการสอน/สร้างนักวิจัยใหม่)
     ได้นำบางส่วนของเนื้อหาด้านการสั่นสะเทือนของมอเตอร์ในฮาร์ดดิสก์ไดร์ฟในส่วนของเนื้อหาทั่ว ๆ ไป และในส่วนของการทดลองและผลการทดลองอย่างคร่าวๆ ไปสอนและอธิบายให้นิสิตฟังในวิชา การสั่นสะเทือนทางกล ระดับปริญญาบัณฑิต ของคณะวิศวกรรมศาสตร์ จุฬาลงกรณ์มหาวิทยาลัย และเนื้อหาโดยคร่าวได้ถูกนำไปลงเรื่องงานวิจัยที่น่าสนใจ ในวารสาร ช่างพูด ซึ่งเป็นวารสารของคณะฯ
     นอกจากนี้ ยังมีการทำวิจัยที่เกี่ยวเนื่องกับโครงการนี้ โดยให้นิสิตระดับปริญญามหาบัณฑิตทำการศึกษา วิจัย เพิ่มเติมจำนวน 1 คน
3. อื่นๆ

ภาคผนวก

ผลงานตีพิมพ์ในวารสารวิชาการนานาชาติ ที่มี Impact factor

- Statistical Energy Analysis on Vibrational Energy Transmission in Hard Disk Drive Components ในวารสาร Microsystem Technologies เล่มที่ 20 ฉบับที่ 8-9 เดือน สิงหาคม ปี 2014 เลขหน้า 1753-1760 มี Impact factor 0.952.

Statistical energy analysis on vibrational energy transmission in hard disk drive components

Nopdanai Ajavakom & Pinporn Tanthanasirikul

Microsystem Technologies
Micro- and Nanosystems Information Storage and Processing Systems

ISSN 0946-7076
Volume 20
Combined 8-9

Microsyst Technol (2014) 20:1753-1760
DOI 10.1007/s00542-014-2229-1

Springer

Microsyst Technol (2014) 20:1753–1760
DOI 10.1007/s00542-014-2229-1

TECHNICAL PAPER

Statistical energy analysis on vibrational energy transmission in hard disk drive components

Nopdanai Ajavakom · Pinporn Tanthanasirikul

Received: 16 October 2013 / Accepted: 25 May 2014 / Published online: 8 June 2014

Abstract One of the problems found in the 2.5 in. hard disk drives (HDDs) in operation is the vibration of the HDD case. Aiming to find crucial information to reduce the vibration transmitted to the outer shell of HDD, the parameters involving vibrational energy transmission through the main components of HDD are identified by the test-based statistical energy analysis (SEA). First, the vibration tests of HDD in the idle mode are performed in order to identify the contribution of the main components; the top cover, the platters, and the actuator arm to the overall vibration of HDD. The SEA parameters including the dissipation loss factors of the individual components and coupling loss factors of the pairs of the components are then experimentally determined in order to calculate the vibration transmission power among the components. The determined parameters, hence, provide some vibrational energy transmission characteristics to facilitate the design of the HDD components to generate less vibration. With some further studies using this concept, the vibration due to shock exerted to the shell of HDD that is transmitted to main components inside the HDD can also be reduced.

1 Introduction

A hard disk drive (HDD) is a primary storage device of every computer. With high demand in a quieter operation of HDDs, and very little or no perceived vibration to the user, the manufacturers want to reduce vibration of the outer case of the HDD as much as possible. Thus, the study of vibration of the HDD and its main components is needed. Shen (2000) reviews some vibration issues in HDDs including vibration of disk/spindle system and the relations between its natural frequencies and the rotational speed. Tandon et al. (2006) look into the vibration and acoustic noise of HDDs operating at various rotational speeds. They study vibration of platters through their natural frequencies by analytical, numerical, and experimental methods at various rotating speeds and the effect of the distance between the actuator head and the disk to the vibration of HDD. It is found that the two major sources of noise are the actuator arm and the platter air fluttering noise of the platters.

Vibration of HDD is originated from the moving components inside HDD especially the spindle motor and the platters (Shen 2000; Tandon et al. 2006). This vibration is then transmitted to the base of the motor, which is manufactured as the same piece as the back case of HDD, and then transmitted to the top cover. To reduce the transmitted vibration to the outer case of HDD, the vibration of the source itself and/or the vibration transmission from the source to the destination should be suppressed as much as possible. Focusing on the later, the vibration energy transmission from the source to the connected components can be determined by many approaches, for example the numerical structural intensity technique by Xu et al. (2004) on disks, the spindle motor and the rotor, and the bearing. In this article, the statistical energy analysis (SEA) principle, the compound of the energy knowledge and statistics (Lyon 1975; Sarradj 2004), is applied. SEA has been studied by many researchers and applied to many structures to analyze the vibration and acoustic noise with successful results e.g., structural vibration transmission through a motor vehicle by Steel (1996), acoustic noise and vibration of electric motors by Dalaere et al. (1999), and impact sound transmission in building structures by Kim et al. (2001). It is

N. Ajavakom (✉) · P. Tanthanasirikul
Department of Mechanical Engineering, Faculty of Engineering, Chulalongkorn University, Bangkok 10330, Thailand
e-mail: nopdanai.a@chula.ac.th

Fig. 1 Vibration measuring positions on HDD case

considered to be useful for complex structure because of its easiness and robust (Dalaere et al. 1999; Kim et al. 2001; Lyon 1975; Sarradj 2004; Steel 1996). Hence, SEA should be a suitable analysis to vibration of a small and complex structure such as the HDD.

This article focuses on study of vibrational energy transmission in HDD components by using SEA. The study starts from finding HDD vibration spectrum to identify how much each main component of the HDD contributes vibrational energy to the exterior of the HDD. The SEA parameters including the dissipation and coupling loss factors are then determined experimentally on 2.5 in. HDDs. The SEA parameters as well as the power transmission spectra are useful sources for a further study to find a way to suppress the vibration. They are not only for the vibration transmitted to the exterior of the HDD, but with some more experiments they are also for reducing of the vibration occurred from the exterior such as the shock that is transmitted to the HDD interior components and it may causing some damage.

2 Contribution of main components of HDD to vibration

A HDD consists of many major components, which are the top cover, the platters, the spindle motor, the actuator arm set with read and write heads and a back case. Each component contributes to the overall HDD vibration at different frequencies and different intensity of vibration. In order to identify the contribution of the three main components, the top cover, the platter set (platters and a rotor), and actuator arm set to the vibration of the HDD, the vibration tests are performed on identical 2.5 in. HDDs. Two corners of the HDD shown in Fig. 1 are measured for their acceleration signals when the HDDs are operating in the idle mode. The diagram of the experimental set-up is shown in Fig. 2 showing a tachometer and an accelerometer as sensors and a digital signal analyzer as a vibration signal analyzer. The acceleration spectra are shown in Fig. 3 in the frequency range of 0–5 kHz showing a highest peak at 90 Hz at an average of 0.665 m/s^2 over the two positions from all HDD samples. In addition, there are some high and dense peaks in the range of 500–2,000 Hz with a maximum point at 0.0173 m/s^2 over the range. The first peak at the spindle rotational speed (90 Hz) is the highest peak of all and also much higher than the others. The peaks in the 500–2,000 Hz range are close to each other meaning that the system is highly damped in this region. By modal testing, these peaks not including 90 Hz are proved to be near HDD natural frequencies.

In order to find the influence of the main components including the top cover, the platters with the rotor and the actuator arm to the overall HDD vibration, the identical vibration tests are performed again when one or more of the components are removed. Seven more cases are carried out as listed in Table 1 where ‘yes’ means the component is present and ‘no’ means the component is removed.

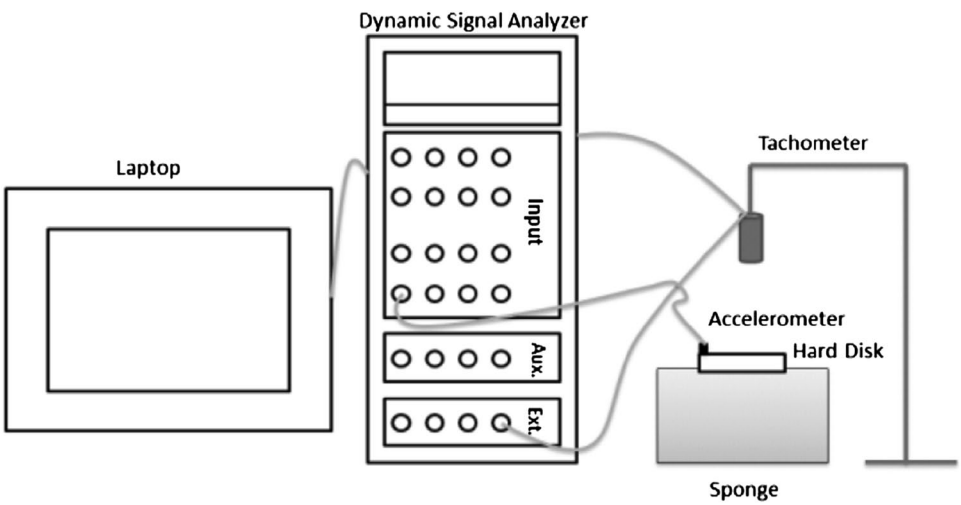

Fig. 2 Vibration measurement experimental setup

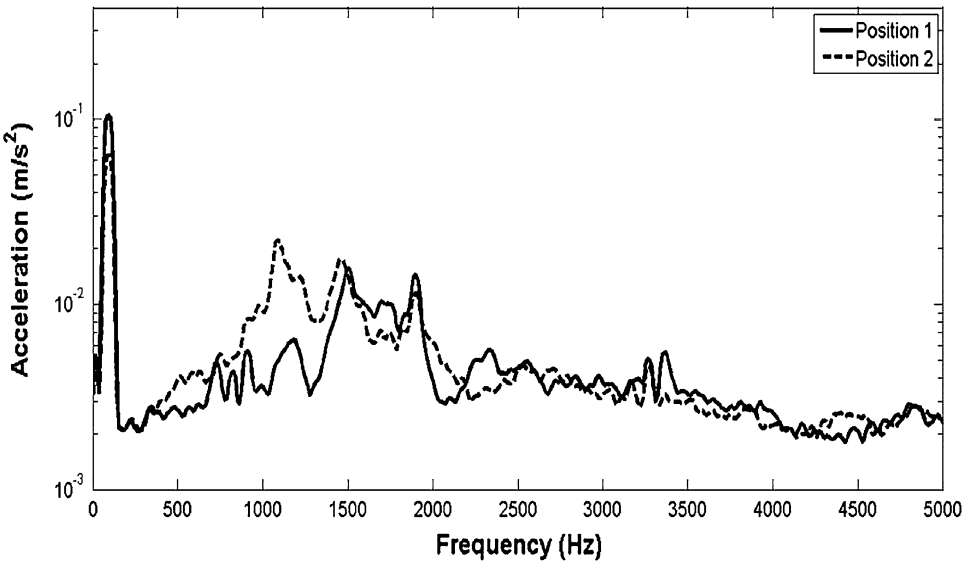

Fig. 3 HDD vibration spectra at two positions on HDD

Table 1 Eight cases of HDD vibration tests

Case	Top cover	Platter set	Actuator arm
1	Yes	Yes	Yes
2	No	Yes	Yes
3	No	No	Yes
4	No	Yes	No
5	No	No	No
6	Yes	No	Yes
7	Yes	No	No
8	Yes	Yes	No

Table 2 Hard disk drive vibrational energy of each case

Case	Vibrational energy (nJ/kg)	
	At 90 Hz	500–2,000 Hz
1	24.9	0.150
2	24.3	0.523
3	8.56	0.052
4	22.9	0.600
5	11.6	0.034
6	5.18	0.022
7	11.9	0.021
8	49.7	0.251
Component	Contribution (%)	
Top cover	5	−56
Platter set	67	90
Actuator arm	−32	−4

Case 1 is where all components are included. The average vibrational energies (v^2) of the two positions in Fig. 1 are calculated at 90 Hz and over the highly damped range (500–2,000 Hz) and shown in Table 2. Note that when the cover is removed, the measured positions are at the same corners but without the cover and the screws. In addition, the contributions of the top cover, the platter set, and the actuator arm are computed from the differences of the energies between the cases with and without the component and are shown in Table 2. The results show that the platter set give 67 and 90 % contribution to HDD vibration at 90 Hz and over 500–2,000 Hz range, respectively. On the other hand, the cases with the top cover give less vibration than the cases without it as indicated by a negative contribution value of the top cover over the 500–2,000 Hz range. That is the top cover can actually reduce the HDD vibration by 56 %. At 90 Hz, the top cover contributes only 5 %. Lastly HDD vibration with the actuator arm is 32 % less at 90 Hz and 4 % less over 500–2,000 Hz range than that of HDD without it. In conclusion, the platter set gives the highest contribution among other two components as the presence of the platters makes the vibration of HDD increased substantially.

3 Vibrational energy transmission of hard disk drive by statistical energy analysis

The vibrational energy transmission of HDD from the platter set as the main contributing component of the vibration of HDD to the exterior of HDD components is studied by observing their vibration transmission power obtained from experimental SEA. The HDD is partitioned into three main subsystems: the platter set (Subsystem 1, SS1), the top cover (Subsystem 2, SS2), and the actuator set on the back case with the base of the spindle motor (Subsystem 3, SS3) as shown in Fig. 4.

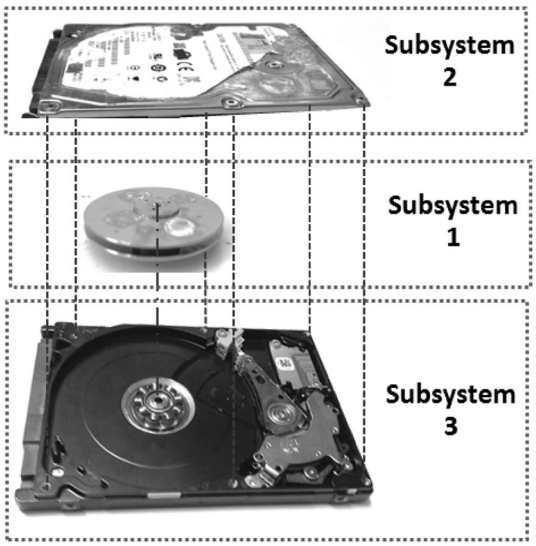

Fig. 4 Three connected subsystems of HDD

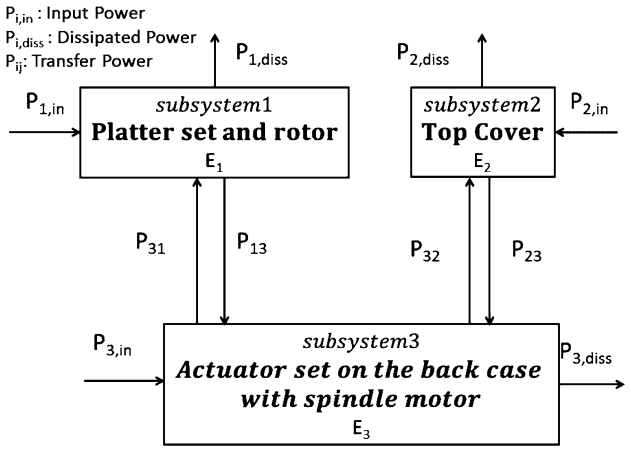

Fig. 5 Three connected subsystems of HDD

3.1 SEA parameters

By the SEA theory, each subsystem is receiving, storing and exchanging energy to one another and the environment. The power flow (the input, the dissipated, and the transfer powers) of the three subsystems is shown in Fig. 5. The input power ($P_{i,\text{in}}$) is the power from the force excited to the subsystem that will raise the subsystem stored energy E_i. The dissipated power ($P_{i,\text{diss}}$) is the power loss to the environment due to energy dissipation (Lyon 1975; Sarradj 2004). The transfer power (P_{ij}) is the power transferred between two subsystems, i.e., from SSi to SSj. Hence, the power equations of SS1, SS2 and SS3 are

$$P_{1,\text{in}} = P_{1,\text{diss}} + P_{13} - P_{31} \tag{1}$$

$$P_{2,\text{in}} = P_{2,\text{diss}} + P_{23} - P_{32} \tag{2}$$

$$P_{3,\text{in}} = P_{3,\text{diss}} + P_{31} + P_{32} - P_{13} - P_{23} \tag{3}$$

The dissipation loss factor of SSi (η_i), the dissipation of the stored energy in SSi to the environment, is the ratio of dissipated power and average stored energy of the subsystem (Lyon 1975):

$$\eta_i = \frac{P_{i,\text{diss}}}{\omega E_i}, \tag{4}$$

where ω is the frequency. The coupling loss factor between SSi and SSj (η_{ij}), a parameter representing the characteristics of the transferring energy between the coupled subsystems, can be determined from Lalor's (1990):

$$\eta_{ij} \approx \frac{1}{\omega}\frac{E_{ji}}{E_{ii}}\frac{P_{j,in}}{E_{ij}}, \tag{5}$$

where E_{ji} is the vibrational energy of SSi when SSj is excited. The transfer power from SSi to SSj can be calculated from

$$P_{ij} = \omega\,\eta_{ij}\,E_i. \tag{6}$$

Transmission power ($P_{ij,\text{net}}$) between subsystems is the net the transfer power between each subsystem:

$$P_{ij,\,\text{net}} = P_{ij} - P_{ji}. \tag{7}$$

3.2 SEA parameters determination

Experiments are performed on HDD samples to determine the SEA parameters: the dissipation loss factors (η_i) and the coupling loss factors (η_{ij}). The transmission power from the platter set (SS1) to the back case (SS3) (i.e., $P_{13,\text{net}}$) and then from the back case (SS3) to the top cover (SS2) (i.e., $P_{32,\text{net}}$) are then determined. In Fig. 6, each subsystem is placed on the sponge where the input force, the acceleration, and the velocity are measured. The dynamic signal analyzer working with a computer collects and analyzes the data, and also displays the results. Using input power technique (Lyon 1975), the input power (P_{in}) at the excited position and the average stored energy (E_i) (determined from the mean square of velocities over the surface area of the subsystem) are used to complete Eq. (4) to find the dissipation loss factors shown in Fig. 7. The complete HDD is then put to test on the sponge in place of a subsystem. The coupling loss factors of the pairs of subsystems, which are the pair of SS1 and SS2 and the pair of SS1 and SS3, are then determined by sub-experiments that give the energies (E_{ji}, E_{ii}, and E_{jj}) and the power (P_j) in Eq. (5). The four coupling loss factors are depicted in Fig. 8. Finally, the transmission powers from SS1 to SS3 ($P_{13,\text{net}}$) and from SS3 to SS2 ($P_{32,\text{net}}$) computed from Eqs. (6) and (7) are shown in Fig. 9.

The dissipation loss factors in Fig. 7 of the subsystems tell their vibration characteristics how much stored energy will be dissipated at a frequency. It is found that they tend

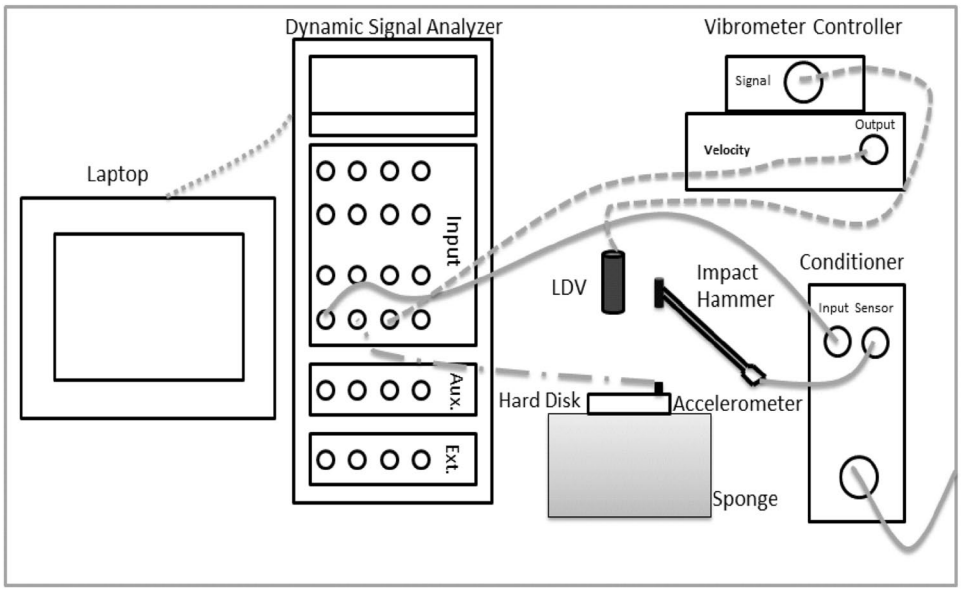

Fig. 6 SEA experimental setup

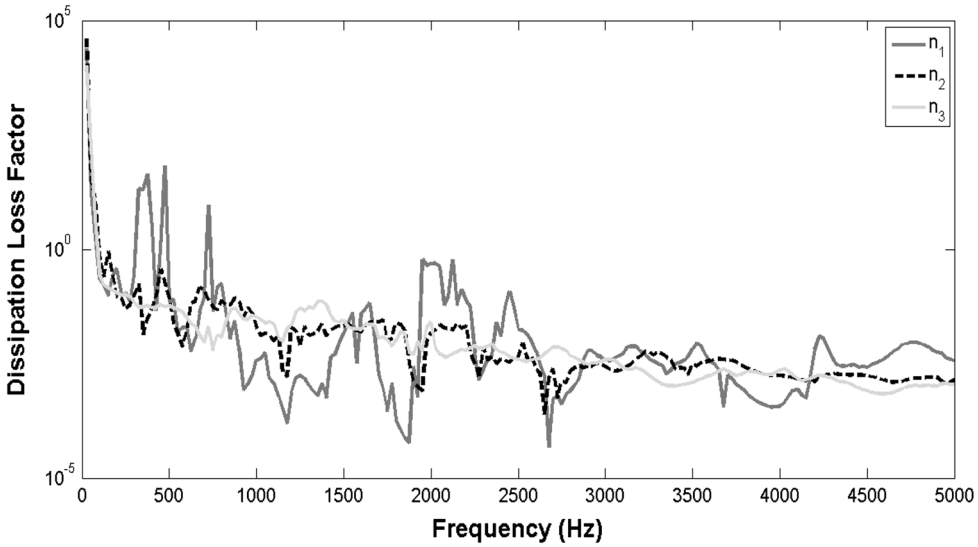

Fig. 7 Dissipation loss factors

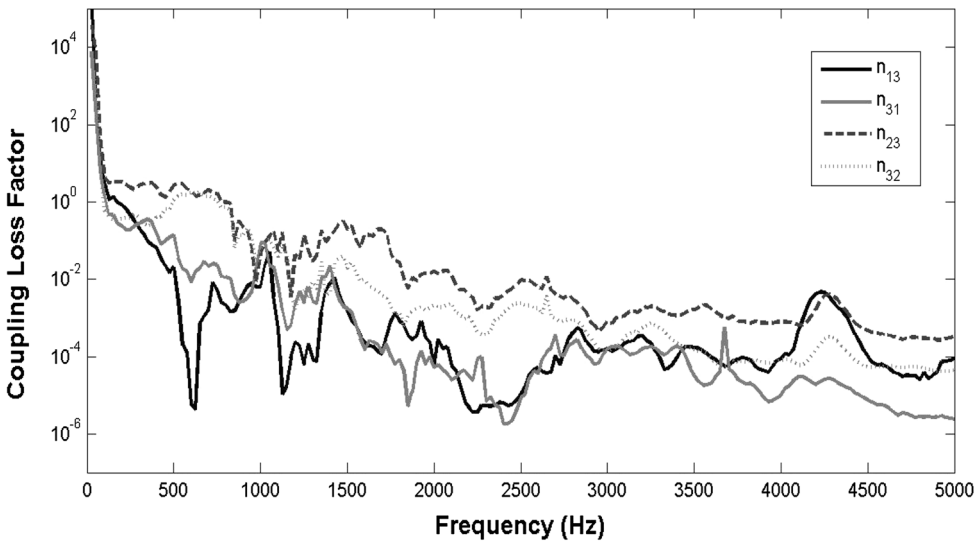

Fig. 8 Coupling loss factors

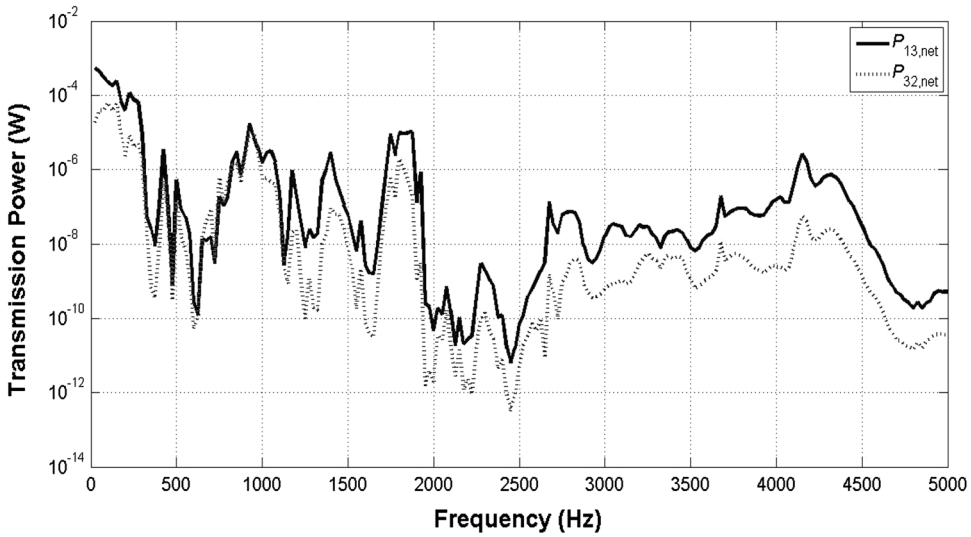

Fig. 9 Transmission powers

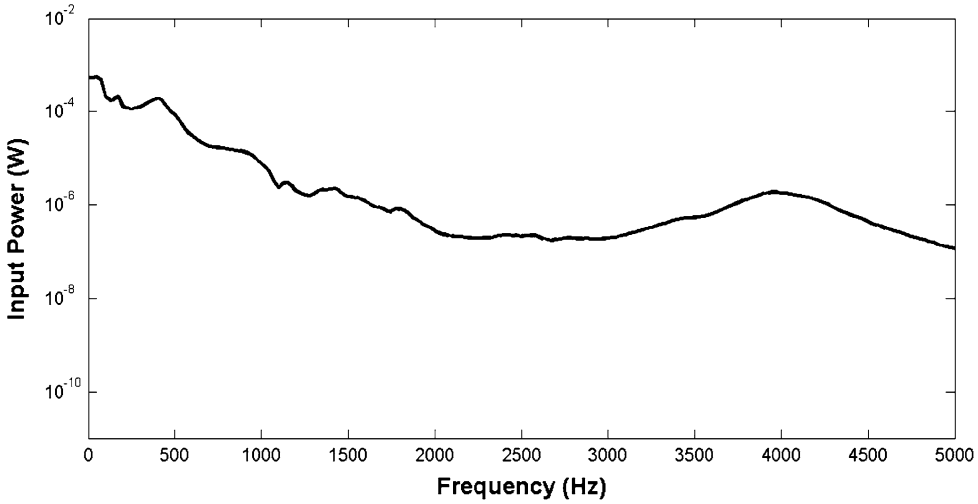

Fig. 10 Input power at SS1

Table 3 Vibrational energies of SS1 and SS3

Sub system	Overall vibrational energy (J)		Difference (%)
	Actual	Calculated by SEA	
1	4.55×10^{-6}	2.47×10^{-7}	94.6
3	4.86×10^{-6}	8.27×10^{-6}	70.2

to be inversely proportional to their frequency response functions (FRF) especially near the natural frequencies where the dissipation loss factors drop substantially while the FRF shows high peaks. The coupling loss factors in Fig. 8 of the pairs of subsystems tell how much the energy will transfer from one subsystem to the other. The high peaks of the coupling loss factors is observed to be close to subsystems' natural frequencies as the energy transfer rises near these frequencies. Furthermore, it can be observed from Fig. 9 that the net vibrational power transmitted from SS1 to SS3 is more than that from SS3 to SS2 over the whole range i.e., there is more power transmitted from platters to the back cover than that from the back cover to the top cover. In addition, the peaks of the transmission power spectra occur at almost the same frequencies as those peaks in vibration spectrum from vibration test (Fig. 3) especially the first four peaks approximately at 90, 1,000, 1,400, and 1,700 Hz. i.e., more power is transmitted where the vibration amplitude is high.

3.3 SEA parameter verification

In order to verify the SEA parameters that have been identified from the prior experiments, input power is given to SS1 (Fig. 10) and the calculated and actual vibrational energy outputs of SS1, SS3 are then compared and shown

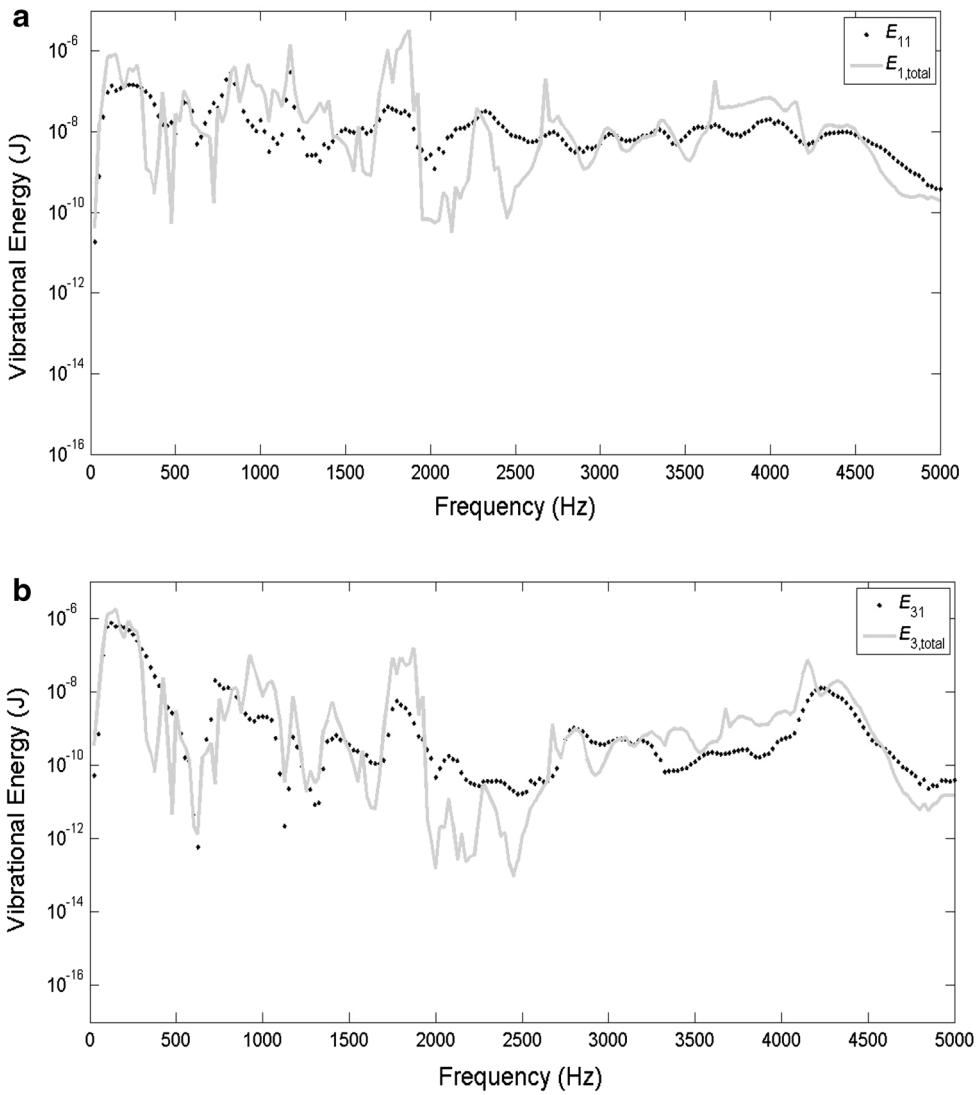

Fig. 11 **a** Calculated (E_{1total}) and actual (E_{11}) energies of SS1 and **b** calculated (E_{3total}) and actual (E_{31}) energies of SS3

in Table 3 and Fig. 11. Figure 11 shows the vibrational energies of SS1 and SS3 resulted from the input at SS1 where the solid lines are the SEA calculated energies (E_{1total} and E_{3total}) (i.e., E_{3total} is E_3 calculated from Eqs. 1, 2, 3 and 4) and the dotted lines are the actual vibrational energies (E_{11} and E_{31}) (i.e., from measured velocities of various points of the system). It can be observed from the figure that the calculated one and the actual one are acceptably close with 94.6 and 70.2 % difference for SS1 and SS3, respectively.

4 Conclusions

Vibration of the HDD is studied in two parts. The first part is to identify the contribution of the components to HDD vibration through the vibration testing of HDDs. The measured vibration spectra show that the platter set is the main contributor of HDD vibration especially at the platters' rotational speed 90 Hz. The second part is to determine the transmission of the vibrational energy from one component to other components through SEA. The SEA parameters, which are dissipation loss factor and coupling loss factor, of the three subsystems: the platters, the top cover, and the actuator set on the back case with the spindle motor, are identified from the experiments. The calculated transmission energies between two pairs of subsystems show that the vibration transmitted power between the platter set and the back case is higher than that between the top cover and the back case, and also the vibrational power is transferred much at the frequencies with high magnitude of HDD vibration especially at resonance. The results from the study can be used as the HDD component vibration characteristics to help reduce the vibration of HDD by decreasing the transmission of the vibrational energy from the platter set to the other components.

Acknowledgments This work is supported by Thailand Research Fund (MRG53) and Mechanical Engineering department, Faculty of Engineering, Chulalongkorn University.

References

Dalaere K, Iadevaia M, Heylen W, Sas P, Hameyer K, Belmans R (1999) Statistical energy analysis of acoustic noise and vibration for electric motors: transmission from air gap field to motor frame. Proc IEEE Ind Appl Soc 34:1879–1902

Kim MJ, Kim HS, Sohn JY (2001) Prediction and evaluation of impact sound transmission in apartment building structures by statistical energy analysis (SEA). Appl Acoust 62:601–616

Lalor N (1990) Practical considerations for the measurement of internal and coupling loss factors on complex structures. ISVR Technical Report No. 1

Lyon RH (1975) Statistical energy analysis of dynamical systems: theory and applications. The MIT Press Cambridge, London

Sarradj E (2004) Energy-based vibroacoustics: SEA and beyond. Gesellschaft für Akustikforschung Dresden mbH, Dresden

Shen IY (2000) Recent vibration issues in computer hard disk drives. J Magn Magn Mater 209:6–9

Steel JA (1996) The prediction of structural vibration transmission through a motor vehicle using statistical energy analysis. J Sound Vib 193(3):691–703

Tandon N, Agrawa VP, Rao VVP (2006) Vibration and noise analysis of computer hard disk drives. Meas 39:16–25

Xu XD, Lee HP, Lu C (2004) Numerical study on energy transmission for rotating hard disk systems by structural intensity technique. Int J Mech Sci 46:639–652